Acta Cryst. (1997). D**53**, 703–712

Lysozyme Aggregation Studied by Light Scattering. II. Variations of Protein Concentration

YANNIS GEORGALIS,* PATRICK UMBACH, JANNIS RAPTIS AND WOLFRAM SAENGER

Institut für Kristallographie, Freie Universität Berlin, Takustrasse 6, Germany. E-mail: yannis@chemie.fu-berlin.de

(*Received 30 December 1996; accepted 6 May 1997*)

Abstract

Static and dynamic light scattering have been employed to investigate the behaviour of nucleating lysozyme solutions in the range between 0.34 and 3.08 m*M*. Preselected concentrations of NaCl and $(NH_4)_2SO_4$ have been used to screen the repulsive Coulombic interactions and trigger aggregation. Initially, mass-fractals undergoing diffusion limited-like aggregation coexist with monomers or small lysozyme oligomers. The growth kinetics of the fractals deliver observables that exhibit distinct tendencies when examined as a function of lysozyme concentration. The behaviour of the observables changes drastically around 2.0 m*M* lysozyme. Static light scattering experiments revealed progressive restructuring or growth of compact structures at later stages of the aggregation. Based on the correlations between the observables an attempt is made to predict whether the examined solutions will crystallize or not. A tentative scheme, involving the most prominent structures observed in nucleating lysozyme solutions, is discussed.

1. Introduction

The work described in this paper is connected closely with our previous studies (Georgalis, Zouni, Eberstein & Saenger, 1993; Georgalis & Saenger, 1993; Georgalis, Schüler, Eberstein & Saenger, 1994; Eberstein, Georgalis & Saenger, 1993, 1994), and is especially close to part I which is the preceding paper in this issue of *Acta Cryst.* (Georgalis, Umbach, Raptis & Saenger, 1997). In part I we investigated the aggregation behaviour of lysozyme at a constant concentration of lysozyme, 1.03 m*M*, which renders crystallization suboptimal within the range of examined electrolyte concentrations.

In the present work, the previous studies are extended to determine the optimal crystallization conditions of the enzyme. The aggregation events were monitored by dynamic light scattering (DLS) and static light scattering (SLS) as previously described. In DLS experiments, we reproducibly observe at least two particle populations, the first representing lysozyme monomers (or oligomers) and the second mass-fractal clusters (van Dongen & Ernst, 1985*a*,*b*), more widely known as amorphous precipitate. The two populations are interconnected through equilibrium conditions and coexist with other species that are not always resolved by DLS.

The lysozyme concentration was varied but the concentrations of electrolytes were held fixed. They were chosen to be above the turnpoints determined in our previous work (Georgalis *et al.*, 1997). The growth kinetics suggest that lysozyme aggregates are mass-fractal clusters. The same set of observables is deduced from the kinetics, and an interconnection between them is attempted. Optimal crystallization conditions are expected within a narrow range of lysozyme concentrations at the given electrolyte concentrations. According to our findings, fractals play a central role in nucleating solutions. A tentative scenario of the events observed during lysozyme crystallization is discussed at the end of this work.

2. Materials and methods

Lysozyme preparation and aspects concerning SLS and DLS are identical to those previously reported (Georgalis *et al.*, 1997). In the present work, lysozyme concentration was varied between 0.34 and 3.08 m*M*. $(NH_4)_2SO_4$ and NaCl were employed at fixed concentrations of 1.10 and 0.70 *M*, respectively. The chosen conditions correspond to those that allow crystal formation long after completion of DLS experiments and absence of considerable multiple scattering, for at least few hours. All solutions were buffered with 0.1 *M* Na acetate buffer, pH 4.25, and experiments were conducted at 293 (±1) K.

3. Results and discussion

Our motivation is to test whether and how fractal cluster growth can be correlated to the nucleation process. Only very recently, and after applying contemporary aggregation theory, could we establish semi-quantitative empirical relations between the effectiveness of crystallization and the observables (Georgalis *et al.*, 1993; Georgalis & Saenger, 1993; Georgalis *et al.*, 1994; Georgalis, Schüler, Frank, Soumpasis & Saenger, 1995) deduced by time-resolved DLS. An assumption in the discussion below is that pre-critical nuclei formation occurs nearly immediately after protein and electrolyte are

mixed, within the dead times of the experiment (nucleation burst). These nuclei, due to repulsive interactions, fail to organize into lattices and collide with each other to form fractal aggregates. Only a minority of the nuclei attains the critical size and promotes crystal formation. This assumption is qualitatively supported by the experiments and it will be discussed in more detail later.

In nucleating lysozyme solutions, monomers (or smaller oligomers) coexist with large fractal clusters and the DLS spectra are dominated by their presence because of the (nearly) fourth-power weighting of the radius. The two populations can be decoupled from each other by inverse Laplace transformation. Precise decoupling of additional populations with intermediate radii and number densities (*i.e.* nuclei) is in principle possible but difficult.

Time-resolved DLS allows for the determination of (i) the radius of the small oligomeric species with radius R_m. The latter correspond to the stationary component that appears in the correlograms. It is determined as an average over all spectra in a kinetic experiment. If their scattering amplitudes allow (*i.e.* they do not get completely consumed by other processes), their mean radius can be precisely determined. (ii) The fractal dimension of the clusters, d_f. (iii) The zero-time extrapolated cluster radius, $R_h(0)$, and (iv) the 'quasi-stationary' hydrodynamic radius, R_h^{qs}, taken as an average radius of all records between 30 and 35 min (*i.e.* when the kinetics have levelled off). (v) Tentative estimates of the sticking probability on impact, α, which typifies aggregation (*cf.* equation 1).

In Fig. 1 the radii of the monomers (or oligomers), R_m, are displayed as a function of lysozyme concentration. The radii of these oligomers increase with increasing protein concentration for both electrolytes. In the presence of $(NH_4)_2SO_4$, Fig. 1(*a*), the radii of the oligomers increase up to 3.5 nm in a way that could correspond to a continuous association. Assuming a compact spatial arrangement of the monomers, these oligomers may resemble dimers to tetramers. If aggregation is induced by NaCl the oligomers exhibit similar behaviour but their radius does not exceed some 2.50 nm as shown in Fig. 1(*b*). The data can be represented by a linear dependence on lysozyme concentration, for both electrolytes. For $(NH_4)_2SO_4$ the coefficients of the fit are: $b_0 = (1.96 \pm 0.1)$ and $b_1 = (5.45 \pm 0.05) \times 10^{-1}$, and for NaCl $b_0 = (1.92 \pm 0.03)$ and $b_1 = (1.88 \pm 0.07) \times 10^{-1}$. Note that for both electrolytes R_m at infinite dilution extrapolates close to the radius of the lysozyme monomer, 1.96 nm. Following considerations similar to those in our previous work (Georgalis *et al.*, 1995, 1997) we can conclude that sufficient amounts of stable dimers, with a radius of 2.73 nm, are present in both electrolytes for triggering crystallization.

In Fig. 2 we display the aggregation kinetics of lysozyme at constant electrolyte concentration. Repeated experiments suggested standard errors that did not exceed 15%. Fitting was accomplished with a DLCA-like power-law model,

$$R_h(t) = R_h(0)(1 + \alpha c_S t)^{z/d_f}, \quad c_S = \frac{4k_BT}{3\eta} N_0, \quad (1)$$

where $R_h(0)$ serves as an estimate of the minimum aggregate radius at time zero and z is an exponent set equal to 1. c_S denotes the Smoluchowski rate constant, k_BT the thermal energy, η the viscosity of the solvent and N_0 the number of monomers at time zero. The factor α denotes the sticking probability of collision between clusters. For ideal DLCA kinetics $\alpha = 1$, for other type of kinetics it is much smaller than unity (Sonntag & Strenge, 1987). An exponential type of kinetics, corresponding to reaction-limited cluster–cluster aggregation (RLCA), was not justified by the data.

The slope of the kinetics delivers the reciprocal fractal dimensions, d_f, Fig. 3, which typifies the morphology of the aggregates (Lin *et al.*, 1989*a*,*b*). If aggregation is induced by $(NH_4)_2SO_4$ a value of d_f *ca*

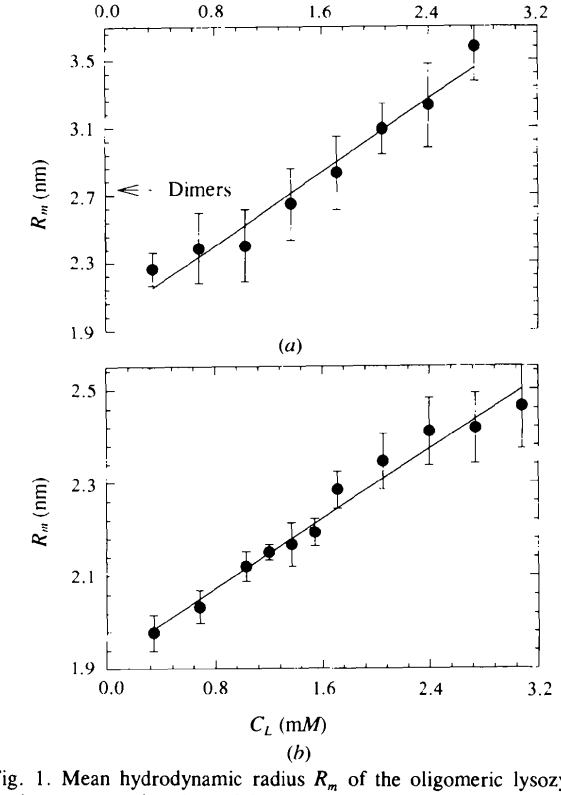

Fig. 1. Mean hydrodynamic radius R_m of the oligomeric lysozyme clusters as a function of lysozyme concentration for (*a*) 1.1 M $(NH_4)_2SO_4$ and (*b*) 0.70 M NaCl, in 0.1 M Na acetate buffer, pH 4.25 at 293 ± 1 K. Cluster radii resemble dimers to tetramers in (*a*) but do not exceed that of dimers in (*b*), if we assume a spherical shape.

1.85 is obtained only at low lysozyme concentrations and drops linearly with increasing lysozyme concentration, in Fig. 3(*a*). This dependence can be qualitatively understood as follows. An increment of lysozyme concentration results in an increment of the number of collisions (*cf.* equation 1). The fractals are getting larger but were more tenuous, because most collisions occur at their periphery. If aggregation is induced by NaCl, d_f shows a weaker dependence on lysozyme concentration, Fig. 3(*b*). The mean value is $d_f = 1.75$, similar to the value of 1.81 typifying the DLCA regime. For both electrolytes d_f is compatible to that expected for DLCA but lower than expected for pure RLCA ($d_f = 2.10$), monomer–cluster diffusion-limited aggregation (DLA) and monomer–cluster reaction-limited aggregation (RLA) regimes. There, d_f is expected to be equal or larger than 2.50 (Vicsek, 1989).

The intercepts of the fractal growth kinetics (*cf.* equation 1) deliver the zero-time extrapolated radius $R_h(0)$, Fig. 4. One should consider these values only as a tentative upper bound of the radii typifying nuclei (see also discussion on Fig. 10). When aggregation is induced by $(NH_4)_2SO_4$, a plateau at 20 nm is attained above 2.0 m*M* lysozyme, Fig. 4(*a*). If the aggregation is induced by NaCl a clear maximum of 28 nm is observed at comparable lysozyme concentrations, Fig. 4(*b*). These estimates for $R_h(0)$ agree with those determined in previous studies, between 5 and 35 nm, by DLS and small-angle X-ray scattering (SAXS) for comparable conditions (Georgalis *et al.*, 1995). Clusters with radii between 3.0 and 30 nm have also been implied in the data analysis of the small-angle neutron scattering (SANS) study by Niimura, Minezaki, Ataka & Katsura (1995).

If aggregation is induced by $(NH_4)_2SO_4$ we notice that $R_h(0)$ remains well below 30 nm, a radius that could correspond to the post-critical nuclei. Simultaneously, the fractal dimension drops from 1.84 to 1.55, Fig. 3(*a*), and R_h^{qs} increases from 0.4 to 2.5 μm. This can be understood as a continuous accumulation of small clusters on fractals that are getting larger, but more tenuous. The system appears then to favour fractal,

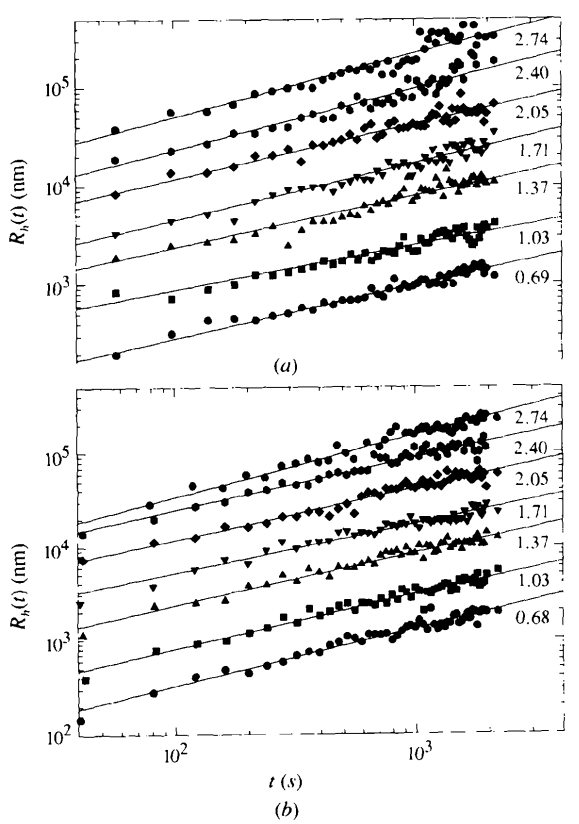

Fig. 2. Typical time-resolved kinetics of lysozyme induced as described in Fig. 1. The mean hydrodynamic radius, $R_h(t)$, of the fractal clusters is plotted as a function of the elapse time of the reaction for (*a*) 1.1 *M* $(NH_4)_2SO_4$ and (*b*) 0.70 *M* NaCl. The number designating each curve denotes m*M* of lysozyme. The linearity of the plots corroborates DLCA-like aggregation. For the sake of clarity the curves are displaced by ascending powers of 2 from bottom to top.

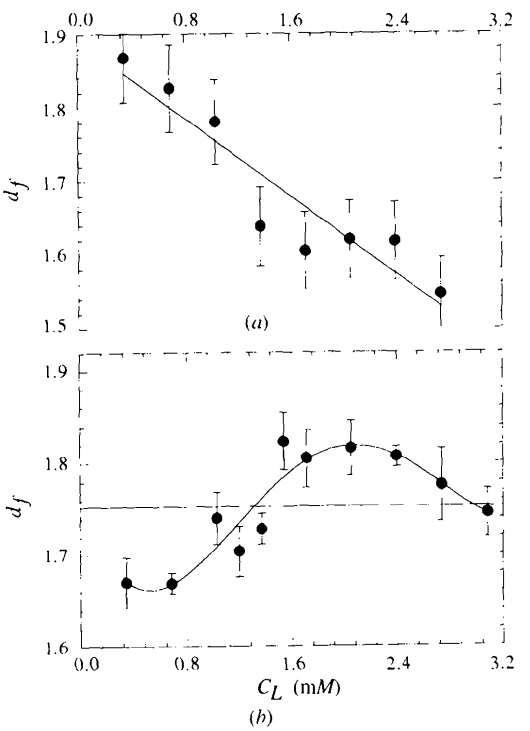

Fig. 3. Fractal dimension d_f plotted as function of lysozyme concentration at (*a*) 1.1 *M* $(NH_4)_2SO_4$ and (*b*) 0.70 *M* NaCl. The continuous drop of the fractal dimension in (*a*) correlates well with the rise of the quasi-stationary hydrodynamic radius, R_h^{qs} displayed in Fig. 5. It signifies that the clusters are getting larger and more tenuous upon collisions with smaller clusters in their periphery. The fractal dimension of clusters obtained with NaCl, (*b*), exhibits a weak dependence on lysozyme concentration (well above experimental error); we are reluctant to attribute significance to this behaviour. The mean fractal dimension, 1.75, resembles closely the theoretically expected value for DLCA, 1.81. The curves through the points serve only as guides to the eye.

more than crystal formation.* Gel formation is observed, after a few days, above 2.0 mM lysozyme.

Clear differences can be ascertained when comparing the quasi-stationary radii, R_h^{qs}, of the clusters evolving in each electrolyte, Fig. 5. If aggregation is induced by $(NH_4)_2SO_4$, R_h^{qs} increases linearly up to 2.5 μm at 2.8 mM lysozyme,† Fig. 5(*a*). In this case, the continuous accumulation of nuclei on fractals favours gel formation. In contrast, when aggregation is induced by NaCl, R_h^{qs} reaches a plateau of 1.7 μm above 2.0 mM lysozyme, Fig. 5(*b*). Slightly below this lysozyme concentration, at 1.55 mM, the system is driven against crystallization. The origin of the saturation of R_h^{qs} can be understood if we assume that the fractals do not grow larger since most of the nuclei are consumed for promoting crystal formation.

In Fig. 6 we display approximate estimates of the sticking probability α as a function of lysozyme concentration using values of R_h^{qs}, $R_h(0)$ and d_f determined above (*cf.* equation 1). For both electrolytes, α drops from 0.5 in a monotonic fashion and reaches a saturation value of 0.115 at 1.30 and 1.60 mM lysozyme for $(NH_4)_2SO_4$ and NaCl, respectively. The saturation value is nearly one order of magnitude lower than that theoretically expected for rapid DLCA.* Interestingly, the lysozyme concentration around the point where α changes slope, resembles that of the optimal crystallization conditions, when aggregation is induced by NaCl (Georgalis *et al.*, 1995).

Since the fractals grow rapidly to sizes exceeding those that can be captured by DLS, their further growth was examined by SLS. Typical experiments are displayed in Fig. 7. Because of space considerations

* A gel can be understood as a large fractal which grows until it fills the whole volume (van Dongen & Ernst, 1985*a*,*b*). An extensive study of the gelation events during the crystallization of lysozyme is given elsewhere (Umbach, Georgalis & Saenger, 1997). † One may think that these radii are beyond the sizes captured by DLS. However, this is not the case; the radii are magnified by a factor of *ca* 1.7 due to an empirical correction applied for decoupling cluster rotational motions (Lindsay, Klein, Weitz, Lin & Meakin, 1988, 1989).

* That α relaxes, for both electrolytes, to the same value seems to be a mere coincidence.

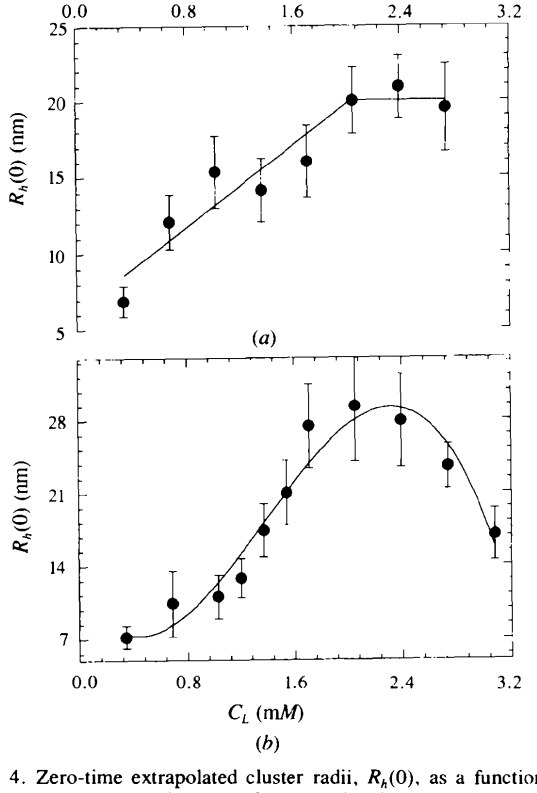

Fig. 4. Zero-time extrapolated cluster radii, $R_h(0)$, as a function of lysozyme concentration. (*a*) If aggregation is induced by 1.10 M $(NH_4)_2SO_4$, $R_h(0)$ increases smoothly to a maximum radius of 20 nm at around 2.0 mM lysozyme. (*b*) If aggregation is induced by 0.70 M NaCl, $R_h(0)$ exhibits a distinct maximum at 28 nm at the same lysome concentration. The latter conditions are reproducibly found to resemble those of optimal lysozyme crystallization (Georgalis *et al.*, 1995). The curves through the points serve only as guides to the eye.

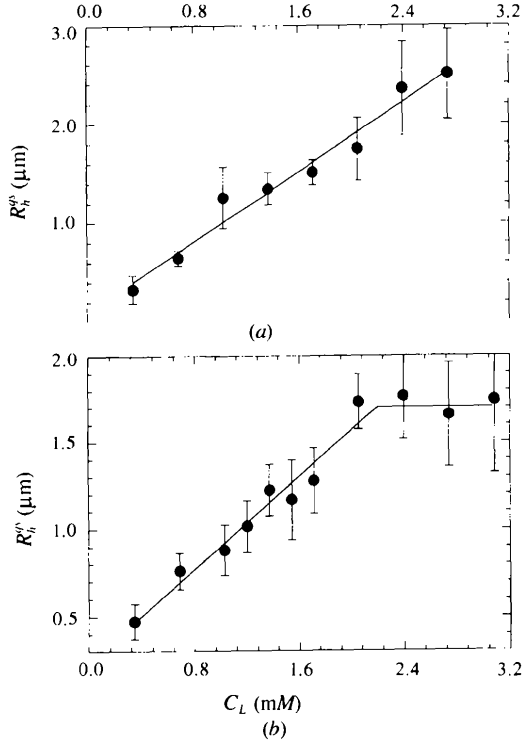

Fig. 5. Quasi-stationary radius R_h^{qs} plotted as function of lysozyme concentration. (*a*) Aggregation induced by 1.10 M $(NH_4)_2SO_4$ and (*b*) by 0.70 M NaCl. The radii of the clusters at comparable lysozyme concentrations are in (*a*) clearly larger than those in (*b*). The latter reach a plateau of 1.7 μm above 2.0 mM lysozyme. The saturation can be qualitatively understood as a preference of nuclei to form microcrystals than incorporate to fractals. The curves through the points serve only as guides to the eye.

only three lysozyme concentrations have been studied at electrolyte concentrations corresponding to those employed for the DLS experiments. Scattered intensities were collected in the angular range between 15 and 110° with a resolution of 2.5°. They were acquired faster than those previously reported (Georgalis *et al.*, 1997); the duration of integration was only 10 s at each angle, and a larger photomultiplier aperture was used.

The intensity distributions exhibit the behaviour expected for mass fractals (Lin *et al.*, 1989*a*,*b*; Schaefer, Bunker & Wilcoxon, 1990). As in our previous work, the conclusions drawn from conventional SLS are only qualitative unless aggregation proceeds in the power-law regime. The relevant property is the fractal dimension of the clusters which can be deduced from the asymptotic scaling behaviour of the intensity distribution,

$$\langle I(q)\rangle \propto q^{-d_f} \quad \text{if} \quad qR_g \gg 1, \tag{2}$$

where q denotes the scattering vector,

$$q = \frac{4\pi n}{\lambda}\sin\left(\frac{\theta}{2}\right), \tag{3}$$

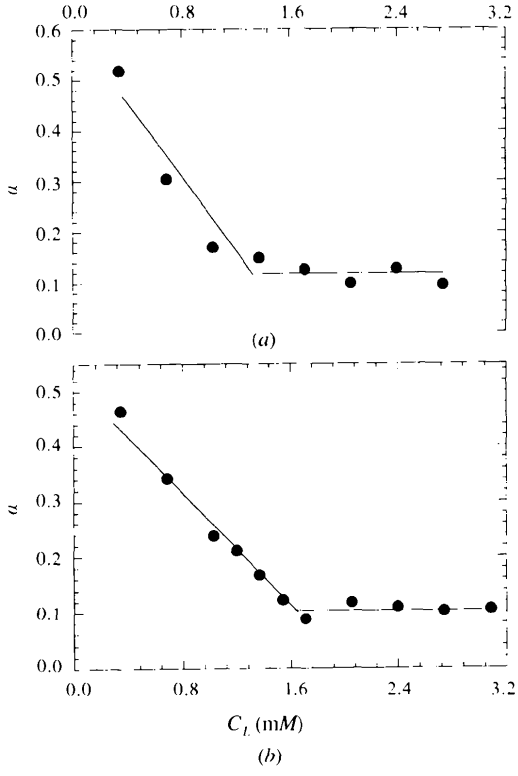

Fig. 6. Tentative estimates of the sticking probability, computed from equation (1), and plotted as a function of lysozyme concentration. Note that α drops initially from values lower than theoretically predicted for DLCA and reaches a saturation value of 0.115 for both electrolytes at comparable lysozyme concentrations of *ca* 1.6 mM. The curves through the points serve only as guides to the eye.

that depends on the index of refraction of the medium, n, on the radiation wavelength, λ, and on the scattering angle θ; R_g denotes the cluster radius of gyration. Within the range of the examined scattering vectors, the power-law regime is attained within the first 20 min of aggregation with both electrolytes. The dimensionalities of the first records are compatible to those obtained from the DLS experiments. The solid lines on each data set ($d_f = 3$) suggest that compact clusters evolve within one hour.* This behaviour implies that either restructuring of the fractals or parallel growth of compact components (*i.e.* nuclei) prevails after these times (see also discussion on Fig. 9).

The SLS data obtained with $(NH_4)_2SO_4$, deserve some discussion. The bell-shaped records at higher lysozyme concentrations (Figs. 7*b*,*c*) signify a competition between fast aggregation and the times required for the photomultiplier to complete an angular scan.† For solutes exhibiting low polydispersity we can account for this effect employing the scattered intensities recorded by a second detector, placed at 270°, to normalize the intensities. However, this approach may be not always applicable in the examined nucleating systems if polydispersity is high. Therefore, the scattered intensities before aggregation enters the power-law regime, should be considered only qualitatively.

4. Interconnection between the observables

We will examine below the global features that associate the observed tendencies for R_h^{qs}, $R_h(0)$ and R_m which are interconnected *via* the sticking probability of collision α (*cf.* equation 1) which depends on the interparticle interactions, described by the potential of mean force (PMF) between the charged monomers. The behaviour of the PMF computed for the lysozyme–NaCl system is however, not monotonic and the interplay between packing and electrostatics cannot be expressed in simple terms (Soumpasis & Georgalis, 1997). These computations have shown the development of an increasing repulsive barrier with increasing NaCl concentration and monomer aggregation occurs only in a 'window' of electrolyte and protein concentrations.

The behaviour of R_h^{qs} and α can be discussed as follows. An increment of the monomer concentration is expected to increase the aggregation rates, so that larger fractals grow at equivalent times (compare Figs. 5 and 6). However, at constant electrolyte concentration, a diminishes with increasing lysozyme concentration and saturates when sufficient repulsion, from salt-mediated

* As previously mentioned (Georgalis *et al.*, 1997) direct comparisons between the fractal dimensions obtained by time-resolved DLS and SLS experiments should not be attempted. † The appearance of the peak can be associated with the evolution of long-range structure formed under these conditions. An account of these effects is in preparation.

barriers, counterbalances packing. The interplay between packing and electrostatics, which is the most probable cause of the observed tendencies, cannot be predicted by the classical DLVO (Derjaguin–Landau–Verwey–Overbeek) theory (Verewy & Overbeek, 1948), and PMF computations are required for predicting these effects. They provide at present the only working scheme at high particle and high electrolyte concentrations.

R_h^{qs} and $R_h(0)$ closely correlate with each other when simultaneoulsy plotted as a function of protein and NaCl concentration (Georgalis *et al.*, 1995). Both observables exhibit maxima around 1.55 mM lysozyme and 0.50 M NaCl. In the present study, $R_h(0)$ and R_h^{qs} show a comparable tendency, at lysozyme concentrations around 2.0 mM, $R_h(0)$ is at a maximum (Fig. 4*b*) and R_h^{qs} reaches a plateau (Fig. 5*b*). Interconnecting $R_h(0)$ and R_h^{qs} at the maximum implies that larger nuclei form comparatively large fractal clusters at equivalent times assuming a constant fractal dimension and moderate changes of the sticking probability, Figs. 3(*b*) and 6(*b*).

The behaviour of $R_h(0)$ and R_m imply, in contrast to our previous study where lysozyme concentration was chosen to be suboptimal (Georgalis *et al.*, 1997), favourable crystallization conditions for the lysozyme–NaCl system. This has been verified by microscopy; we reproducibly observe, above 1.55 mM lysozyme and at 0.70 mM NaCl, large tetragonal lysozyme crystals within two days. In contrast, for the lysozyme–$(NH_4)_2SO_4$ system crystallization is again prohibited by a gelling transition indicated by the continuous growth of the fractals increasing with lysozyme concentration (Fig. 5*a*).

5. Dynamic scaling of fractal clusters

In Fig. 8 we display the time-resolved data of Fig. 2 plotted against the dimensionless product $c_S t$ (*cf.* equation 1). All experiments collapse on a single master

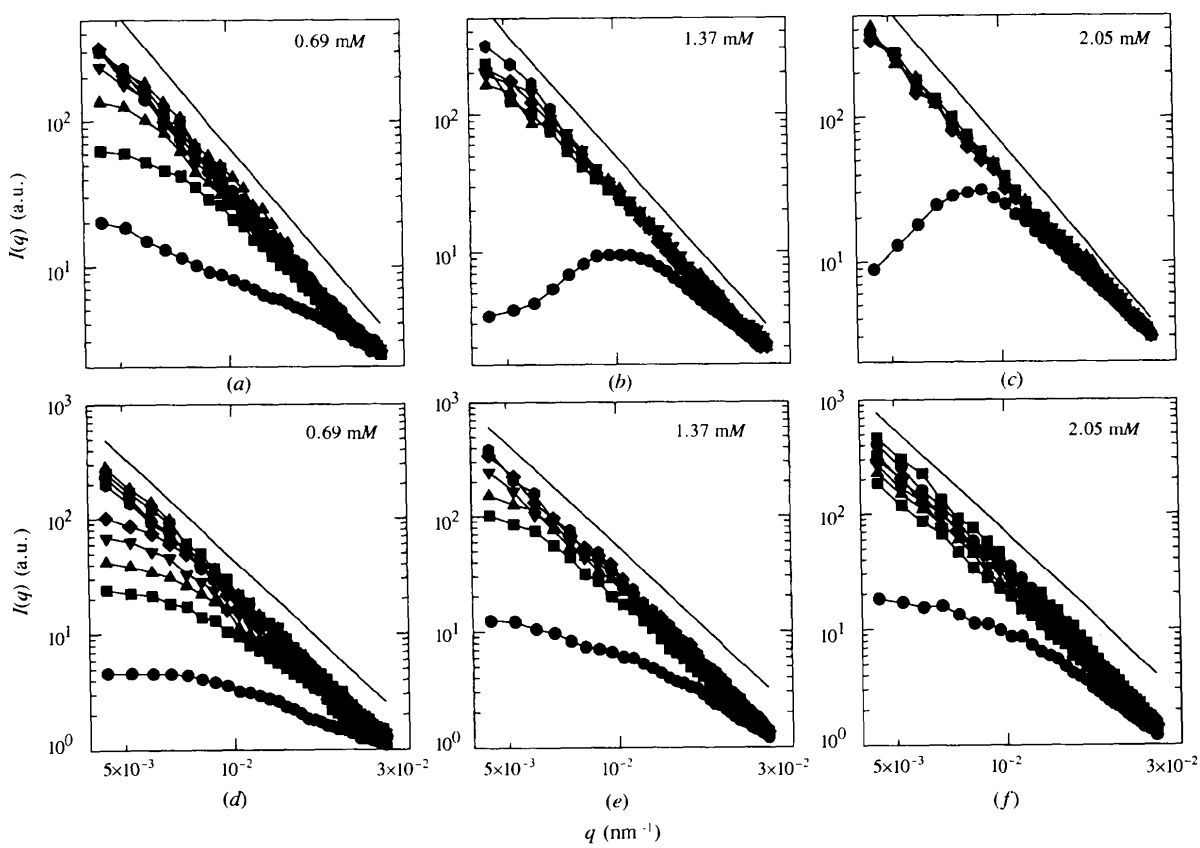

Fig. 7. Normalized SLS scattered intensities plotted as a function of scattering vector. The electrolyte concentration was 1.10 M $(NH_4)_2SO_4$ in (*a*), (*b*) and (*c*) and of 0.70 M NaCl in (*d*), (*e*) and (*f*). The respective lysozyme concentrations are in (*a*) and (*d*) 0.69 mM, (*b*) and (*e*) 1.37 mM and (*c*) and (*f*) 2.05 mM, other experimental conditions are given in Fig. 1. Scattered intensities were collected in the angular range between 15 and 110°. Note the progressive increase of the slopes as a function of time required to complete an angular scan (symbols typify angular scans of *ca* 20 min). Dimensionalities compatible to those obtained by DLS is obtained from the asymptotic region of the first record and gradually increase to higher values. The latter can be understood either as restructuring of the fractal clusters or as increment of the number of coalescing species in solution with time (nuclei). The solid line, included for comparison, indicates the evolution of compact clusters ($d_f = 3$ *cf.* equation 2).

curve with a reciprocal slope corresponding to the fractal dimension, d_f. For $(NH_4)_2SO_4$ induced aggregation, d_f is 1.80 ± 0.05 and for NaCl-induced aggregation it is 1.78 ± 0.02. The dynamic scaling is a property obeyed by colloidal fractal clusters (Klein *et al.*, 1990). It should be noted that changes of the sticking probability (Fig. 6) within an order of magnitude from unity, do not influence appreciably the dynamic scaling of the fractals.

Scaling with concentration has also been shown by Ataka & Asai (1990) to hold for crystallizing lysozyme solutions but in a different context. It signifies the colloidal character of the clusters developing in nucleating protein solutions and poses the question whether the formation of fractal structures is an unavoidable step towards nucleation. If the interactions between monomers are non-specific, the case most often encountered with proteins, long times will be required for proper alignment to ordered structures. Therefore, fractal formation seems more probable than nucleation, at least at the beginning of the reaction. Nucleation may then proceed *via* restructuring of the fractal clusters. This postulate is supported only by few experimental studies (Brune, Romainczyk, Röder & Kern, 1994; Dokter, van Garderen, Beelten, van Santen & Bras, 1995) and for nucleating lysozyme solutions has been investigated by atomic force microscopy in solution (Schaper, Georgalis, Umbach, Raptis & Saenger, 1997).

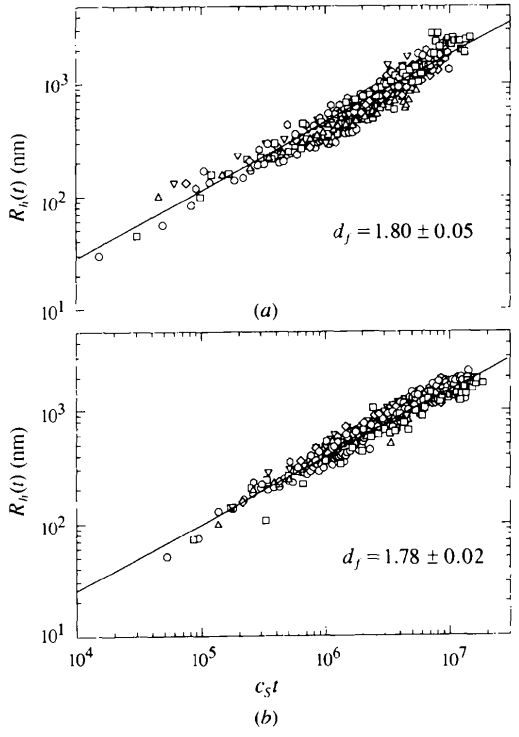

Fig. 8. Time-resolved kinetic experiments (Fig. 2) normalized with the Smoluchowski rate c_S (*cf.* equation 1 assuming $z = 1$). Note that all data sets collapse on a single master curve. The reciprocal slope of the regression line delivers the fractal dimension (*a*) $d_f = 1.80 \pm 0.05$ for aggregation induced with $1.10\,M$ $(NH_4)_2SO_4$ and (*b*) $d_f = 1.78 \pm 0.02$ for aggregation induced with $0.70\,M$ NaCl.

6. Sedimentation of fractals by gravity

Components underlying particle size distributions may often be hidden because of their unfavourable weighting in the scattered intensity. Only prevailing particle populations, either because of their size or number density or both, will then be captured. Since the contribution of the larger fractals dominates the scattering, one possibility is to wait long enough, until they sediment and recover scattering from the smaller species.

In Fig. 9 we display a selected experiment involving $2.05\,mM$ lysozyme incubated with $0.70\,M$ NaCl. Whereas the sequence of events during the first hour is very similar to that described above, there are some new features which appear when the fractals sediment, after five days. We have detected four species; their mean hydrodynamic radii are plotted semi-logarithmically as a function of q^2.

The main features of these experiments can be summarized as follows. (i) The radii of the monomeric or oligomeric species remain practically unchanged at

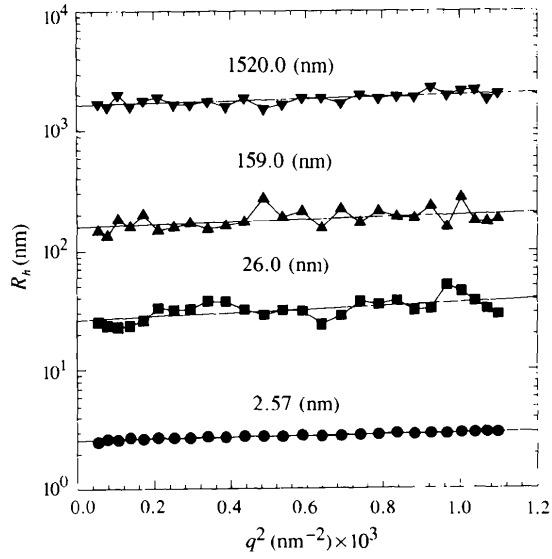

Fig. 9. Angular dependence of the hydrodynamic radii of the components present in a $2.05\,mM$ lysozyme solution incubated with $0.70\,M$ NaCl. Other conditions are identical to those of Fig. 1. Observations were in the angular range between 15 and 110°. All four components were resolved by Laplace-inverting the spectra as previously described (Georgalis *et al.*, 1993, 1995). The quoted radii correspond to $q \rightarrow 0$ estimates and were deduced after allowing five days for the fractals to sediment. There is no appreciable angular dependence for any of the detected species.

2.57 nm (compare with Fig. 1). (ii) The 'invisible' population with radii of 26.0 nm (compare with Fig. 4) becomes now 'visible' and persists for several days in solution. These sizes corroborate the estimates deduced for $R_h(0)$. (iii) A population, not previously detected, with radii of around 159 nm and (iv) fractals with radii close to 1.5 μm. After five days, the latter are present in the solutions however, at lower amounts than at the beginning of the experiment, as roughly judged from the respective DLS amplitudes (data not shown).

Different events will be observed when nucleating solutions are clarified by centrifugation prior to measurements, and thus willingly or unwillingly one removes the fractals. This is more a matter of persuasion than taste. We always use uncentrifuged solutions since they more closely resemble the crystallization attempts in the laboratory. The nucleation reaction usually proceeds quite fast and fractals with radii of 500 nm typically form within 5 min. It is pointless to discuss what happens in a centrifugal field. One should remember that typical initial monomer number concentrations are roughly 10^{18} particles (per cm^3). By removing 10^6 fractals (tentative estimates at optimal conditions) involving 10^6 monomers one removes in practice 10^{12} particles. Subtracting 10^{12} from 10^{18} particles makes no real difference; and will escape detection by standard UV absorption techniques. Therefore, one might conclude that there are no losses before and after the centrifugation of nucleating solutions. This is incorrect as the removal of 10^{12} particles from an aggregating solution will drastically modify the kinetics, through reduction of the Smoluchowski rate constant, c_S, which is directly proportional to the number of seeding particles, N_0 (*cf.* equation 1). The observed kinetics persist even after repeated filtration and shearing of the fractals and removal of substantial number of particles from the solutions, indicating that all components are associated through equilibrium conditions.

7. A tentative crystallization scenario for lysozyme

We have summarized the most obvious structures observed in nucleating lysozyme solutions in Fig. 10. Under suboptimal crystallization conditions, monomeric lysozyme undergoes Brownian motion in solution, (*A*). Upon addition of electrolyte, the nucleation burst occurs within fractions of seconds. This can be understood as the onset of a catastrophic aggregation. Populations of oligomers are formed at the early stages of the nucleation reaction (*B*). The mean hydrodynamic radius of the oligomers depends strongly on the nature and concentration of electrolyte and on the initial monomer volume fraction, *i.e.* on the potential of mean force that governs the interactions between particles. If the interplay between packing and electrostatics allows, the oligomers will associate further to form nuclei (*C*), which in turn will aggregate to either form random fractals (*E*) or organize to a lattice and form micro- and later macrocrystals (*D*). Finally, for lysozyme percolation of fractals and gelling transitions, (*F*), may be observed depending on conditions. We have therefore to cope with nearly all known Smoluchowski aggregation kernals involving non-gelling and gelling reactions and small–large or large–large cluster collisions (van Dongen & Ernst, 1985*a*,*b*).

Rigorous statements cannot be made for steps (*A*) to (*E*), *i.e.* formation of fractals from monomers. In diffusion-limited monomer–cluster aggregation (DLA),

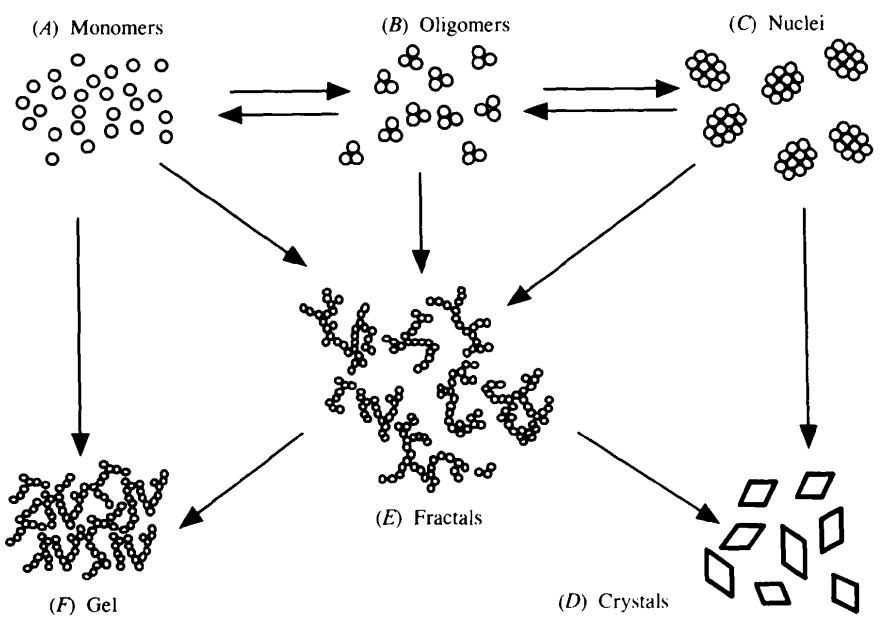

Fig. 10. Pictorial representation of structures involved in the crystallization of lysozyme with a simple electrolyte. (*A*) monomeric lysozyme, (*B*) oligomers, (*C*) nuclei and (*E*) fractals are observed in the early reaction stages. Later, macroscopic crystals (*D*) or gels of various densities may appear, (*F*). The step leading from fractals (*E*) to crystals (*D*) remains questionable where restructuring reflects a challenging possibility. For explanations associating the various steps with each other see text. No attempts should be made at present to associate the indicated steps with specific properties of the solution like pH or temperature. More detailed descriptions of the individual steps should await further experiments.

the hydrodynamic radii are expected to scale on time with an exponent $1/d_f = 2.5$ (Vicsek, 1989). We have not observed such large exponents, but one should be aware of the fact that the exponent characterizing the aggregation kinetics is not $1/d_f$ and z/d_f (*cf.* equation 1). The values of the dynamic exponent z are deliberately set to unity, whereas deviations cannot be excluded as the reaction proceeds (Umbach *et al.*, 1997). The backward reaction for this step seems improbable, and the reversibility between steps (*B*) and (*C*) in Fig. 10 should depend on the terminal size of nuclei. If the nuclei do not reach their critical size, they should redissolve. If they grow to a critical size and escape the Smoluchowski fractal 'sink', crystal growth *via* coalescence is expected to take place. The step from (*E*) to (*D*) can still occur after aimed restructuring of the fractal clusters. However, restructuring is difficult to prove experimentally. Thus, only an average picture can be obtained by conventional SLS. As shown in Fig. 7 however, this mechanism remains a challenging possibility. There is only limited experimental evidence that supports this step and SLS data should be considered, with some caution, as a first indication towards such a mechanism.

From the energetic point of view and at low concentrations, equilibrium is expected to favour fractal cluster (amorphous) rather than crystalline (organized) structure formation. Optimal crystallization conditions should shift the thermodynamic equilibrium from (*C*) to (*D*) keeping the backward rates from (*C*) to (*B*) and the forward reaction rates from (*C*) to (*E*) as low as possible. Our simplified model distinguishes from earlier ideas (Kam, Shore & Feher, 1978; Feher & Kam, 1985) where nucleation is treated as a monomer and (globlar) cluster association process. While essential events may have been captured by this theory, the authors determined only time-independent changes of the diffusion coefficient as a function of electrolyte [in a manner similar to Eberstein *et al.* (1994) and Muschol & Rosenberger, (1995)]. Our findings suggest that fractal formation at concentrations usually employed for crystallization almost always accompanies nucleation; this is valid not only for lysozyme but for all proteins examined in our laboratory. We should stress at this point that the protein concentration regime explored is much below the concentrations required for the observation of protein liquid–liquid or liquid–solid phase transition (Ishimoto & Tanaka, 1977; Thomson, Schurtenberger, Thurston & Benedek, 1987; Taratuta, Holschbach, Thurston, Blankschtein & Benedek, 1990). In the latter regimes, crystal formation is nearly immediate through direct rapid coalescence, and fractal cluster formation is observed neither by small-angle SLS nor by high-resolution optical microscopy (at least in the examined spatial scales). However, because of the high nucleation rates, many but very small crystallites are formed, which are unsuitable for X-ray diffraction purposes.

8. Concluding remarks

The conclusions drawn from the present work are still far from being rigorous. Even in the simplest cases examined, one is confronted with an aquarium of species, sizes or degrees of compactness that vary as a function of protein and electrolyte concentration. Rationalizing this wealth of information is a prerequisite towards a better understanding of protein–protein interactions *per se* and development of intelligent high-capacity crystallization screening techniques. DLS as a first platform offers a size assessment of the species involved in a nucleating solution. Auxiliary techniques like small-angle SLS and diffusion wave spectroscopy (Weitz & Pine, 1993) are used for probing either the very early or the late stages of nucleation reactions of highly concentrated lysozyme solutions.

An open problem is the determination of the relative concentrations of the individual species. Conventional SLS measures only an amplitude-weighted contribution of each species present in solution and one is usually unable to deconvolute the individual contributions. Laplace inversion techniques, with state of the art detection schemes, help to separate several components that underlie the size distribution of nucleating solutions. The amplitudes of these components, as determined by DLS, are less credible and more difficult to deduce than the respective radii. The events observed in typical diagnostic experiments are interconnected in a way that does not allow for simplified considerations. Unless the relative concentrations of the individual species can be determined within a reasonable error frame (say within one order of magnitude), a rigorous theoretical description of the events should await further developments.

The global conclusions emerging from the studies conducted on lysozyme is that a detailed knowledge of the aggregation events over wide spatiotemporal scales is necessary. Since the spatial scales involved in the nucleation process are broad, measurements at a single scattering angle inevitably carry minimal information. We believe that the developments mentioned above will have a strong impact on the issue of high-capacity crystallization screening. Understanding the plethora of events present in a simple aggregating system like lysozyme–NaCl will require research at different levels of complexity. Recent observations indicate that more general phenomena might apply to crystallizing systems, not previously considered. While at present several improvements on methodological, technical and computational aspects are required, the perspectives seem promising.

Financial support to YG from the Deutsche Forschungsgemeinschaft (Sa 196/26-1) and to PU from the DESY 05 641KEB project is acknowledged.

References

Ataka, M. & Asai, M. (1990). *Biophys. J.* **58**, 807–811.

Brune, H., Romainczyk, C., Röder, H. & Kern, K. (1994). *Nature (London)*, **369**, 469–471.

Dokter, W. H., van Garderen, H. F., Beelen, T. P. M., van Santen, R. A. & Bras, W. (1995). *Angew. Chem.* **107**(1), 122–125.

van Dongen, P. G. J. & Ernst, M. H. (1985*a*). *J. Phys. A Math. Gen.* **18**, 2779–2793.

van Dongen, P. G. J. & Ernst, M. H. (1985*b*). *Phys. Rev. Lett.* **13**, 1396–1399.

Dubin, S. B., Clark, N. A. & Benedek, G. B. (1971). *J. Chem. Phys.* **54**, 5158–5163.

Eberstein, W., Georgalis, Y. & Saenger, W. (1993). *Eur. Biophys. J.* **22**, 359–366.

Eberstein, W., Georgalis, Y. & Saenger, W. (1994). *J. Cryst. Growth*, **143**, 71–78.

Feher, G. & Kam, Z. (1985). *Methods Enzymol.* **114**, 77–112.

Fisher, M. E. & Burford, R. J. (1967). *Phys. Rev. A*, **156**(2), 583–622.

Georgalis, Y. & Saenger, W. (1993). *Adv. Colloid Interface Sci.* **46**, 165–183.

Georgalis, Y., Schüler, J., Eberstein, W. & Saenger, W. (1994). *Fractals in the Natural and Applied Sciences*, edited by M. M. Novak, pp. 139–151. North-Holland: Elsevier Science.

Georgalis, Y., Schüler, J., Frank, J., Soumpasis, D. M. & Saenger, W. (1995). *Adv. Colloid Interface Sci.* **58**, 57–86.

Georgalis, Y., Umbach, P., Raptis, J. & Saenger, W. (1997). *Acta Cryst.* D**53**, 691–702.

Georgalis, Y., Zouni, A. Eberstein, W. & Saenger, W. (1993). *J. Cryst. Growth*, **126**, 245–260.

Handbook of Chemistry and Physics (1984–1985). Cleveland, Ohio. The Chemical Rubber Co.

Ishimoto, C. & Tanaka, T. (1977). *Phys. Rev. Lett.* **39**(8), 474–477.

Kam, Z., Shore, H. B. & Feher, G. (1978). *J. Mol. Biol.* **123**, 539–555.

Klein, R, Weitz, D. A., Lin, M. Y., Lindsay, H. M., Ball, R. C. & Meakin, P. (1990). *Progr. Colloid Polym. Sci.* **81**, 161–168.

Lin, M. Y., Lindsay, H. M., Weitz, D. A., Ball, R. C., Klein, R. & Meakin, P. (1989*a*). *Nature (London)*, **339**, 360–362.

Lin, M. Y., Lindsay, H. M., Weitz, D. A., Ball, R. C., Klein, R. & Meakin, P. (1989*b*) *Proc. R. Soc. London Ser. A*, **423**, 71–87.

Lindsay, H. M., Klein, R., Weitz, D. A., Lin, M. Y. & Meakin, P. (1988). *Phys. Rev. A*, **38**(5), 2614–2626.

Lindsay, H. M., Klein, R., Weitz, D. A., Lin, M. Y. & Meakin, P. (1989). *Phys. Rev. A*, **39**(6), 3112–3119.

Muschol, M. & Rosenberger, F. (1995). *J. Chem. Phys.* **103**(24), 10424–10432.

Niimura, M., Minezaki, Y., Ataka, M. & Katsura, T. (1995). *J. Cryst. Growth*, **154**, 136–144.

Schaefer, D. W., Bunker, B. C. & Wilcoxon, J. P. (1989). *Proc. R. Soc. London Ser. A*, **423**, 35–53.

Schaper, A., Georgalis, Y., Umbach, P., Raptis, J. & Saenger, W. (1997). *J. Chem. Phys.* In the press.

Soumpasis, D. M. & Georgalis, Y. (1997). *Biophys. J.* In the press.

Sonntag, H. & Strenge, K. (1987). *Coagulation Kinetics and Structure Formation*. Berlin: VEB Deutscher Verlag der Wissenschaften.

Taratuta, V. G., Holschbach, A., Thurston, G. M., Blankschtein, D. & Benedek, G. B. (1990). *J. Phys. Chem.* **94**, 2140–2144.

Thomson, J. A., Schurtenberger, P., Thurston, G. M. & Benedek, G. B. (1987). *Proc. Natl Acad. Sci. USA*, **84**, 7079–7083.

Umbach, P., Georgalis, Y. & Saenger, W. (1997). *J. Am. Chem. Soc.* Submitted.

Vicsek, T. (1989). *Fractal Growth Phenomena*. Singapore: World Scientific.

Verwey, E. J. W. & Overbeek, J. Th. G. (1948). *Theory of the Stability of Lyophobic Colloids*. Amsterdam: Elsevier.

Weitz, D. A. & Pine, D. J. (1993). In *Dynamic Light Scattering, the Method and Some Applications*, edited by W. Brown, pp. 652–720. Oxford Science Publications.